Available online at www.sciencedirect.com
SCIENCE DIRECT®
International Journal of Thermal Sciences 45 (2006) 706–715
International Journal of Thermal Sciences
www.elsevier.com/locate/ijts

Gray radiative conductive 2D modeling using discrete ordinates method with multidimensional spatial scheme and non-uniform grid

Kamal A.R. Ismail *, Carlos T.S. Salinas

Department of Thermal and Fluids Engineering, Faculty of Mechanical Engineering, PO Box 6122, State University of Campinas, 13083-970 Campinas SP, Brazil

Received 30 December 2004; received in revised form 24 August 2005; accepted 10 October 2005

Available online 20 December 2005

Abstract

The problem of radiation heat transfer coupled with other modes of heat transfer is important in many engineering applications. Some examples are the heat transfer in glass fabrication and in thermal isolation materials. The angular and spatial discretization of the radiative transport equation in the discrete ordinates method (DOM) plays an important role to obtain accurate numerical results. Two high order spatial discretization schemes are used and compared. One spatial discretization scheme is unidirectional and the other is multidimensional interpolating scheme. Different angular quadratures are selected and tested to obtain accurate results with less computational time. The radiative heat transport equation is solved using the conventional procedure of solution for DOM and the algorithm is validated by comparison with literature exact solutions for different two-dimensional cases. The radiative source term in the energy equation is computed from intensities field. The radiative conductive model is validated by comparison with test cases solutions from the literature. Non-uniform grids are implemented for multidimensional spatial scheme and the results are compared with the result of uniform grid showing agreement. Also, the non-uniform grids are tested in cases of high temperature gradients. To accelerate convergence an adequate relaxation factors in radiative heat transport equation and in energy equation are used. The method can be used to handle cases with reflecting boundaries.

Keywords: Radiation conduction; Participating media; Discrete ordinates method

1. Introduction

In many engineering applications, the problem of radiation coupled with other modes of heat transfer is important. The heat transfer in glass fabrication and industrial furnaces are some examples of such applications. It is generally required to solve a multidimensional radiation field using computational techniques. Due to the fact that the reaction rates and density distributions are closely related to the local gas temperature, the influence of radiation heat transfer on the combustion dynamics is very strong and the radiation heat transfer can significantly affect the gas temperature and walls. In practice radiative heat-transfer calculations are complex and consequently many approximate solutions are proposed, including, among others, methods based upon diffusion approximation, the methods of P_n and simplified P_n, the method of discrete ordinates, the method of discrete transfer, and the method of finite volumes.

The Rosseland diffusion equation for radiative energy transfer has the same form as the Fourier law of heat conduction and this allows solution of some radiation problems and is also used for simplified cases in some CFD codes, as Phoenics and CFX. The P_n approximation introduced initially by Krook [1] and Cheng [2] is simply taking the momentum of the radiative transport equation to obtain a system of equations free of the angular dependence. Each P_n approximation results in a system of n^2 equations and in the limit, that is, for large n, the P_n approximation results in the solution of the transport equation.

The method of discrete ordinates DOM is an attractive simplified method to solve radiative transfer problems. This method was originally formulated by Chandrasekhar [3] and developed by Lathrop and Carlson [4] and Lathrop [5]. Fiveland [6,7] formulated an accurate method of discrete ordinates of the first order based upon the method of control volumes for two-dimensional and three-dimensional enclosures and pre-

* Corresponding author. Fax: +55 19 37883213.
E-mail addresses: kamal@fem.unicamp.br (K.A.R. Ismail), csalinas_99@yahoo.com (C.T.S. Salinas).

1290-0729/$ – see front matter
doi:10.1016/j.ijthermalsci.2005.10.004

Nomenclature

A	area	m^2
dx, dy	dimensions of control volume in x and y direction	m
c_p	specific heat	$J\,kg^{-1}\,K^{-1}$
$\mathbf{G}$	non-dimensional incident radiation intensity	
k	thermal conductivity	$W\,m^{-1}\,K^{-1}$
$\mathbf{I}$	radiation intensity	$W\,m^{-2}\,sr^{-1}$
$\mathbf{I}_b$	blackbody radiation intensity	$W\,m^{-2}\,sr^{-1}$
L_x, L_y	dimensions of the cavity in x- and y-direction	m
M	number of discrete directions	
$\mathbf{n}$	unit vector normal to the surface	
N	Planck number	
P	Pressure	$N\,m^{-2}$
$\mathbf{Q}$	dimensionless heat flux	
$\mathbf{q}$	local heat flux per unit area	$W\,m^{-2}$
$\mathbf{q}_r$	net total radiative flux	$W\,m^{-2}$
$\mathbf{r}$	vector position	m
r_x, r_y	parameter of non-uniform grid	
S_{df}	deferred factor correction	
S_r	radiative source term	$W\,m^{-3}$
$\mathbf{S}_{LT}$	radiative source function	$W\,m^{-2}\,sr^{-1}$
T	temperature	K
t	time	s
V	volume	m^3
w	weight of angular quadrature	
x/y	x/y-coordinate	m

Greek symbols

β	extinction coefficient	m^{-1}
β_f	coefficient of thermal volumetric expansion	K^{-1}
ε	total emissivity	
κ	absorption coefficient	m^{-1}
λ	relaxation factor	
ρ	reflectivity	
ρ_f	medium density	$kg\,m^{-3}$
σ	scattering coefficient	m^{-1}
σ_o	Stefan–Boltzmann constant	$W\,m^{-2}\,K^{-4}$
μ	direction cosine	
ξ	direction cosine	
Ω	direction vector	
Θ	non-dimensional temperature	

Subscripts

h/c	hot/cold
i, j	space grid position
$\mathbf{m}$	the mth discrete ordinate

Superscripts

n	iteration number
$\mathbf{m}$	the mth discrete ordinate used for radiative intensity ($\mathbf{I}, \mathbf{S}_{LT}$)

sented general outlines of the method. Viskanta and Menguc [8] used the method in combustion problems, while Ramankutty and Crosbie [9,10] presented a more recent and extensive review and used this method to formulate the so-called modified discrete ordinates. Later, Sakami and Charette [11] applied the modified discrete ordinates using triangular grids and finite elements methods. The techniques of total variation (TVD), presented by van Leer [12] and Hearten [13], were applied by Jessee and Fiveland [14] to solve radiation problems. Based upon the techniques TVD, Jessee and Fiveland [14] formulated a second order interpolation CLAM scheme. Based upon genuinely two-dimensional advection schemes (Sidilkover and Roe [15]), Balsara [16] formulated a new second order scheme with multidimensional interpolation for RTE, and is called genuinely multidimensional (GM), and the resulting non-linear system of equations is solved by using multigrid techniques in conjunction with the Newton–Krylov method.

The selection of angular quadrature is also one important aspect to consider to obtain accurate solutions as in Fiveland [6, 7], Truelove [17], Balsara [16], Thurgood [18] and Koch et al. [19]. One serious drawback of the method is the so-called "ray effect", which is a consequence of angular discretization. As it is explained in Modest [20], if one considers an enclosure with a very small zone of very high emission, the intensity from this zone will be carried away from it into the directions of the discrete ordinates. Far away from the emission zone, these rays may become so far apart that some control volumes and/or surface zones may not receive any energy from this high-emission zone, and hence leading to unphysical results.

Rousse [21] and Rousse et al. [22] used the control volume method for RTE and the finite element method for the energy equation in the solution of conduction–radiation and convection–radiation problems in two-dimensional closed cavities and canals. In their method, the calculation domain is divided in triangular finite elements. Lee and Viskanta [23] compared solutions of combined radiation–conduction heat transfer in two-dimensional semitransparent media using the finite volume method for the energy equation coupling with both DOM and diffusion approximation for RTE. They applied this approach in a glass fabrication problem.

Lacroix et al. [24] used the discrete ordinates method to solve the coupled radiative conductive heat transfer in 2D homogeneous materials such as glass. The media is considered as non-gray absorbing and emitting semitransparent media. In their work a kind of spatial differencing schemes was used and the results for the weighted and the step schemes were presented. Recently, Talukdar and Mishra [25] applied a novel collapsed dimension method for the combined conduction–radiation problem in one-dimensional gray media.

The objective of the present paper is to use an efficient method suitable for working with Cartesian non-uniform grids in 2D situations to solve the RTE and couple the developed code with problems including combined conduction and radiation. In the present study, to handle the problem of radiation–

conduction within two-dimensional enclosure with diffusely emitting and reflecting walls the method of discrete ordinates based upon the method of control volume is used. Also the CLAM scheme and the GM scheme are used for the spatial discretization in conjunction with different angular quadratures. The energy equation is solved using control volume method considering the divergence of the radiant flux vector as one radiative source term. The predictions are validated with other results obtained by different approaches developed by other authors. Uniform and non-uniform grids are implemented, tested, and their convergence and accuracy are compared.

2. Formulation

The energy equation at any location within a radiating medium is given by

$$\rho_f c_p \frac{DT}{Dt} + \nabla\cdot(-k\nabla T) + \nabla\cdot\mathbf{q}_r - q''' - \beta_f T\frac{DP}{Dt} - \phi_d = 0 \tag{1}$$

where $\nabla\cdot\mathbf{q}_r$, the divergence of the radiant flux vector $\mathbf{q}_r$ is considered as a radiative source term; $\frac{D}{Dt}$ is the substantial derivative; β_f is the coefficient of volumetric thermal expansion of the fluid; q''' is the local heat source per unit volume and time, and ϕ_d is the heat production by viscous dissipation.

The energy equation for coupled radiation–conduction heat transfer of an absorbent, emitter and isotropic scatter media, under steady state and with constant thermal conductivity is as in Siegel and Howell [26]:

$$k\nabla^2 T - \nabla\cdot\mathbf{q}_r = 0 \tag{2}$$

Writing the radiative source term as

$$S_r = -\nabla\cdot\mathbf{q}_r \tag{3}$$

The energy equation is

$$k\nabla^2 T + S_r = 0 \tag{4}$$

In two-dimensional Cartesians coordinates, one can write

$$k\frac{\partial^2 T}{\partial x^2} + k\frac{\partial^2 T}{\partial y^2} + S_r = 0 \tag{5}$$

To obtain the temperature distribution in the medium by solving Eq. (5) it is necessary to relate $\nabla\cdot\mathbf{q}_r$ to the temperature radiation distribution within the medium. One approach is to obtain $\nabla\cdot\mathbf{q}_r$ directly by considering the local radiative interaction with a differential volume in the medium. The local divergence of the radiative flux is related to the local intensities by

$$\nabla\cdot\mathbf{q}_r = \kappa\left[4\pi\mathbf{I}_b(\mathbf{r}) - \int_{\Omega=4\pi}\mathbf{I}(\mathbf{r},\boldsymbol{\Omega})\,\mathrm{d}\boldsymbol{\Omega}\right] \tag{6}$$

To obtain the radiation intensity field and $\nabla\cdot\mathbf{q}_r$ it is necessary to solve of the radiative transport equation (RTE). The RTE for an absorbing, emitting gray gas medium with isotropic scattering can be written as in Siegel and Howell [26],

$$(\boldsymbol{\Omega}\cdot\nabla)\mathbf{I}(\mathbf{r},\boldsymbol{\Omega}) = -(\kappa+\sigma)\mathbf{I}(\mathbf{r},\boldsymbol{\Omega}) + \frac{\sigma}{4\pi}\int_{4\pi}\mathbf{I}(\mathbf{r},\boldsymbol{\Omega}')\,\mathrm{d}\boldsymbol{\Omega}' + \kappa\mathbf{I}_b(\mathbf{r}) \tag{7}$$

where $\mathbf{I}(\mathbf{r},\boldsymbol{\Omega})$ is the radiation intensity in $\mathbf{r}$, and in the direction $\boldsymbol{\Omega}$; $\mathbf{I}_b(\mathbf{r})$, is the radiation intensity of the blackbody in the position $\mathbf{r}$ and at the temperature of the medium; κ and σ are the gray medium absorption and scattering coefficients; and the integration is in the incident direction $\boldsymbol{\Omega}'$.

For diffusely reflecting surfaces the radiative boundary condition for Eq. (7) is

$$\mathbf{I}(\mathbf{r},\boldsymbol{\Omega}) = \varepsilon\mathbf{I}_b(\mathbf{r}) + \frac{\rho}{\pi}\int_{n\cdot\Omega'<0}|\mathbf{n}\cdot\boldsymbol{\Omega}'|\mathbf{I}(\mathbf{r},\boldsymbol{\Omega}')\,\mathrm{d}\boldsymbol{\Omega}' \tag{8}$$

where $\mathbf{r}$ belongs to the boundary surface $\boldsymbol{\Gamma}$, and Eq. (8) applies for $\mathbf{n}\cdot\boldsymbol{\Omega}>0$, $\mathbf{I}(\mathbf{r},\boldsymbol{\Omega})$ is the radiation intensity leaving the surface at the boundary condition, ε is the surface emissivity, ρ is the surface reflectivity and $\mathbf{n}$ is the unit vector normal to the boundary surface.

In the method of discrete ordinates the equation of radiation transport is substituted by a set of M discrete equations for a finite number of directions $\boldsymbol{\Omega}_m$, and each integral is substituted by a quadrature series of the form,

$$(\boldsymbol{\Omega}_m\cdot\nabla)\mathbf{I}(\mathbf{r},\boldsymbol{\Omega}_m) = -\beta\mathbf{I}(\mathbf{r},\boldsymbol{\Omega}_m) + \frac{\sigma}{4\pi}\sum_{k=1}^{M}w_k\mathbf{I}(\mathbf{r},\boldsymbol{\Omega}_k) + \kappa\mathbf{I}_b(\mathbf{r}) \tag{9}$$

where w_k are the ordinates weight. This angular approximation transforms the original equation into a set of coupled differential equations, with $\beta=(\kappa+\sigma)$ as the extinction coefficient. Eq. (6) in discrete ordinates is,

$$\nabla\cdot\mathbf{q}_r = 4\pi\kappa\mathbf{I}_b(\mathbf{r}) - \sum_{m=1}^{M}w_m\kappa\mathbf{I}_m \tag{10}$$

Let,

$$\mathbf{S}_m = \frac{\sigma}{4\pi}\sum_{k=1}^{M}w_k\mathbf{I}(\mathbf{r},\boldsymbol{\Omega}_k) \tag{11}$$

where $\mathbf{S}_m$ represents the entering scattering source term.

The two-dimensional radiative transport equation in the $\mathbf{m}$ direction for an emitting, absorbing and scattering medium is

$$\mu_m\frac{\mathrm{d}\mathbf{I}_m}{\mathrm{d}x} + \xi_m\frac{\mathrm{d}\mathbf{I}_m}{\mathrm{d}y} = -\beta\mathbf{I}_m + \kappa\mathbf{I}_b + \mathbf{S}_m \tag{12}$$

where μ_m, ξ_m, are the directional cosines of Ω_m.

The reflection boundary condition in discrete ordinates can be written as

$$\mathbf{I}_m = \varepsilon\mathbf{I}_b + \frac{\rho}{\pi}\sum_{\substack{m'\\ \mu'_m<0}}\mathbf{w}_{m'}|\mu'_m|\mathbf{I}_{m'}, \quad \mu_m>0 \text{ in } x\in\Gamma \tag{13}$$

$$\mathbf{I}_m = \varepsilon\mathbf{I}_b + \frac{\rho}{\pi}\sum_{\substack{m'\\ \xi'_m<0}}w_{m'}|\xi'_m|\mathbf{I}_{m'}, \quad \xi_m>0 \text{ for } y\in\Gamma \tag{14}$$

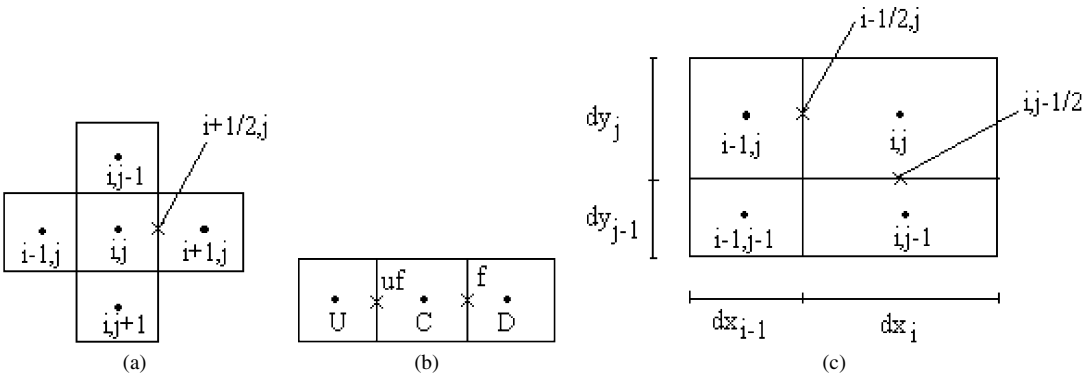

Fig. 1. Interpolation stencil. (a) Volume of control $[i, j]$; (b) CLAM scheme; (c) GM scheme.

The discretization in finite volumes can be obtained by multiplying Eq. (12) by $\mathrm{d}x\,\mathrm{d}y$ and integrating over the control volume (i, j) as in Fig. 1(a)

$$\mu_m A_x\left(\mathbf{I}^m_{i+\frac{1}{2},j} - \mathbf{I}^m_{i-\frac{1}{2},j}\right) + \xi_m A_y\left(\mathbf{I}^m_{i,j+\frac{1}{2}} - \mathbf{I}^m_{i,j-\frac{1}{2}}\right) = V_{i,j}\left[\left(\kappa \mathbf{I}_b - \beta \mathbf{I}^m\right)_{i,j} + \mathbf{S}_m\right] \tag{15}$$

where $V_{i,j}$ is the control volume i, j in m^3.

Assuming that the boundary conditions are given, the system of equations is closed and defines an interpolation system relating the intensities at the face to the nodal values.

3. Interpolation schemes at the faces

In the present work the CLAM scheme of Jessee and Fiveland [14] and the multidimensional scheme (GM scheme) of Balsara [16] are used. In the single direction scheme CLAM, the interpolation in a given face involves three grid nodes and can be represented by three-point scheme as in Fig. 1(b) for the face f. The multidimensional non-linear high order scheme of Balsara [16] so-called genuinely multidimensional (GM), which was used in previous work [27] with uniform grid is now extended for non-uniform grid. The scheme uses the limiting flux technique and the Van Albada limiter, in the form: $Limiter[x, y] = \frac{xy^2+yx^2}{x^2+y^2}$, as proposed by Balsara [16].

For non-uniform Cartesian grid, the following interpolation relations are used to define this scheme (see Fig. 1(c)): for

$$\mu_m \geqslant 0; \quad \xi_m \geqslant 0; \quad \frac{\mu_m}{\mathrm{d}x_{i,j}} \leqslant \frac{\xi_m}{\mathrm{d}y_{i,j}}$$

$$\mu_m \mathbf{I}^m_{i-1/2,j} = \mu_m \mathbf{I}^m_{i-1,j-1} + 0.5\,\mathrm{Limiter}\left[\mu_m\left(\mathbf{I}^m_{i,j} - \mathbf{I}^m_{i-1,j-1}\right) - \mathrm{d}x_{i,j}\mathbf{S}^m_{LT_{i,j}}, \left(\mu_m - \frac{\xi_m\,\mathrm{d}x_{i,j}}{\mathrm{d}y_{i,j}}\right)\left(\mathbf{I}^m_{i-1,j} - \mathbf{I}^m_{i-1,j-1}\right)\right]$$

and

$$\xi_m \mathbf{I}^m_{i,j-\frac{1}{2}} = \xi_m \mathbf{I}^m_{i,j-1} \tag{16}$$

with

$$\mathbf{S}^m_{LT_{i,j}} = -(\kappa_{i,j} + \sigma_{i,j})\mathbf{I}^m_{i,j} + \kappa_{i,j}\mathbf{I}_{bi,j}$$

For

$$\mu_m \geqslant 0; \quad \xi_m \geqslant 0; \quad \frac{\mu_m}{\mathrm{d}x_{i,j}} \geqslant \frac{\xi_m}{\mathrm{d}y_{i,j}}$$

$$\mu_m \mathbf{I}^m_{i-\frac{1}{2},j} = \mu_m \mathbf{I}^m_{i-1,j}$$

$$\xi_m \mathbf{I}^m_{i,j-\frac{1}{2}} = \xi_m \mathbf{I}^m_{i-1,j-1} + 0.5\,\mathrm{Limiter}\left[\xi_m\left(\mathbf{I}^m_{i,j} - \mathbf{I}^m_{i-1,j-1}\right) - \mathrm{d}y_{i,j}\mathbf{S}^m_{LT_{i,j}}, \left(\xi_m - \frac{\mu_m\,\mathrm{d}y_{i,j}}{\mathrm{d}x_{i,j}}\right)\left(\mathbf{I}^m_{i,j-1} - \mathbf{I}^m_{i-1,j-1}\right)\right] \tag{17}$$

For one type of non-uniform grid one can write

$$\mathrm{d}x_{i,j} = r_x\,\mathrm{d}x_{i-1,j} \quad \text{and} \quad \mathrm{d}y_{i,j} = r_y\,\mathrm{d}y_{i,j-1} \tag{18}$$

For the symmetric grid used here for the x and y axes, the values of r_x and r_y are varied between 1.0 to 1.3.

4. Method of solution of RTE

To discretize the radiative transport equation, one can rewrite Eq. (15) based upon the method outlined in Ismail and Salinas [27] as,

$$\left(\mathbf{I}^m_{i,j}\right)^{n+1} = \Big[V_{i,j}(\kappa \mathbf{I}_{bi,j})^n + |\mu_m| A_x \left(I^m_{i-1/2,j}\right)^{n+1} + |\xi_m| A_y \left(\mathbf{I}^m_{i,j-1/2}\right)^{n+1} + V_{i,j}\mathbf{S}^n_m + \mathbf{S}^n_{\mathrm{df}}\Big] \times \left[|\mu_m| A_x + |\xi_m| A_y + \beta V_{i,j}\right]^{-1} \tag{19}$$

Where $\mathbf{S}_m$ is calculate by Eq. (11) and $\mathbf{S}_{\mathrm{df}}$ is the deferred factor correction as calculate in Ismail and Salinas [27]

$$\mathbf{S}^n_{\mathrm{df}} = |\mu_m| A_x \left(\mathbf{I}^m_{i,j} - I^m_{i+1/2,j}\right)^n + |\xi_m| A_y \left(\mathbf{I}^m_{i,j} - \mathbf{I}^m_{i,j+1/2}\right)^n \tag{20}$$

The values of the intensities in the faces $(\mathbf{I}^m_{i+1/2,j})^n$ and $(\mathbf{I}^m_{i,j+1/2})^n$ are interpolated using the CLAM or GM schemes while the values of the intensities $(\mathbf{I}^m_{i-1/2,j})^{n+1}$ and $(\mathbf{I}^m_{i,j-1/2})^{n+1}$ are interpolated using a step scheme.

5. Method of solution of radiative conductive model

To solve the coupled radiation–conduction problem, Eqs. (2) and (6) are converted to non-dimensional form, as in Kim et al. [28],

$$\frac{1}{\tau_{L_x}^2}\frac{\partial^2\boldsymbol{\Theta}(\mathbf{r})}{\partial\mathbf{X}^2}+\frac{1}{\tau_{L_y}^2}\frac{\partial^2\boldsymbol{\Theta}(\mathbf{r})}{\partial\mathbf{Y}^2} = \frac{1-\omega}{\mathbf{N}}\left(\boldsymbol{\Theta}^4(\mathbf{r})-\frac{1}{4}\sum_{m=1}^{M}w_m\mathbf{G}_m\right) \tag{21}$$

With the boundary conditions

$$\Theta(0,Y)=1 \tag{22}$$

$$\Theta(1,Y)=0.5 \tag{23}$$

$$\Theta(X,0)=\Theta(X,1)=0.5 \tag{24}$$

The parameters and non-dimensional variables are

$$X=\beta x/\tau_{Lx},\qquad Y=\beta y/\tau_{Ly}$$

$$\tau_{Lx}=\beta L_x,\qquad \tau_{Ly}=\beta L_y,\qquad \omega=\sigma/\beta$$

$$N=k\beta/4\sigma_o T_h^3,\qquad \Theta=T/T_h,\qquad \mathbf{G}=\mathbf{I}/\sigma_o T_h^4$$

where $\mathbf{G}$ is the non-dimensional incident radiation intensity.

Let, the source term

$$S_r=1-\omega\left(\boldsymbol{\Theta}^4(\mathbf{r})-\frac{1}{4}\sum_{m=1}^{M}w_m\mathbf{G}_m\right) \tag{25}$$

Then the energy equation is

$$\frac{1}{\tau_{L_x}^2}\frac{\partial^2\boldsymbol{\Theta}(\mathbf{r})}{\partial\mathbf{X}^2}+\frac{1}{\tau_{L_y}^2}\frac{\partial^2\boldsymbol{\Theta}(\mathbf{r})}{\partial\mathbf{Y}^2}=\frac{S_r}{\mathbf{N}} \tag{26}$$

After solving the intensities and temperature fields, the heat fluxes can be calculated. The dimensionless directional heat fluxes, $\mathbf{Q}_x$ and $\mathbf{Q}_y$, consist of both conduction and radiation. They are thus defined as in [28]:

$$\mathbf{Q}_x=-\frac{4\mathbf{N}}{\tau_{Lx}}\frac{\partial\boldsymbol{\Theta}}{\partial\mathbf{X}}+\sum_{m}^{M}w_m\mu_m\mathbf{G}^m \tag{27}$$

$$\mathbf{Q}_y=-\frac{4\mathbf{N}}{\tau_{Ly}}\frac{\partial\boldsymbol{\Theta}}{\partial\mathbf{Y}}+\sum_{m}^{M}w_m\xi_m\mathbf{G}^m \tag{28}$$

where the first and second terms on the right-hand side are the dimensionless conductive and radiative heat fluxes.

One can identify the energy equation, Eq. (26) of the problem, as the Fourier conduction equation with one radiative source term. This equation is solved using the control volume method, as in Patankar [29].

The source term linearization is obtained by

$$S_r=S_C+S_P T_P \tag{29}$$

As the radiative source term have a complicated expression in T (i.e., Θ), $S_P=0$ and $S_C=S_r(T_P^*)$ were used, where the symbol T_P^* denotes the previous iteration value of T_P. Due the non-linearities in the discretization equations which may cause large changes in the predicted solutions and produce oscillations and/or divergence in the iteration process, the relaxation technique (Patankar [29]) in the dependent variable is used. To solve the radiative transport equation, over-relaxation is used to accelerate convergence. To solve energy equation it necessary to use relaxation technique specially for the case of non-uniform grid.

The procedure of the numerical calculations starts by assuming that the radiative source term is zero and the energy equation is solved to find the temperature field. The ADI line-by-line method is used to quickly bring the information from all boundaries to the interior. After, the radiative transport equation is solved using DOM until convergence of intensities field is obtained, then the radiative source term is calculated and the energy equation is solved including the source term only once for the global iterative process to permit faster convergency. The iterative process continues until achieving convergence of the intensities radiative field and global iteration and the temperature field. By this procedure, it was not necessary to set chosen temperature at the corners of the enclosure in the hot wall side, for example $T=0.75T_h$ as it is reported in Rousse et al. [22].

The convergence of the solution was evaluated using a convergence criterion taken as the error in the intensity field in RTE solution and the error in the temperature field respectively as,

$$\text{error}\,G=\text{Max}\left|\frac{\mathbf{G}_{i,j}^n-\mathbf{G}_{i,j}^{n-1}}{\mathbf{G}_{i,j}^n}\right|\leqslant 10^{-6}\quad\text{and}$$

$$\text{error}\,T=\text{Max}\left|\frac{\Theta_{i,j}^n-\Theta_{i,j}^{n-1}}{\Theta_{i,j}^n}\right|\leqslant 10^{-5} \tag{30}$$

6. Validation of radiative conductive model

Several numerical experiments were realized to ensure that the algorithm does not have any directional march error or negative intensities. In the case of the GM scheme, the last problem was solved by the careful implementation of Eqs. (16) and (17) and not setting zero for the negative intensities.

A test case of radiation conduction in a square cavity with participating media is solved. Fig. 2 shows a simplified scheme of the cavity. Surface 2 is hot and is at temperature T_h; surfaces 1, 3 and 4 are cold at temperature T_c, that is equal to one half of T_h. The media in cavity is gray and the boundaries are black surfaces. The medium is further assumed to absorb and emit radiation, but not scatter radiant energy, $\omega=0$.

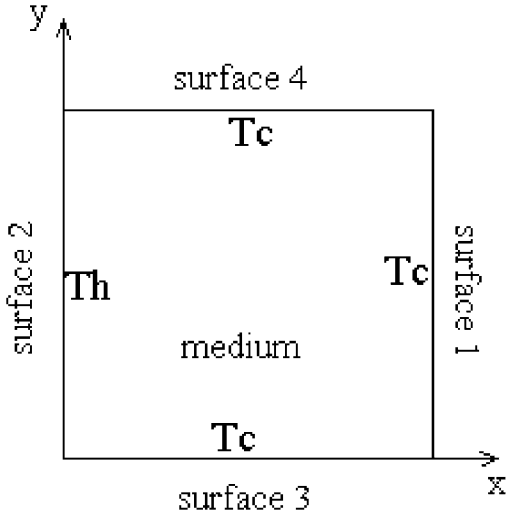

Fig. 2. Two-dimensional cavity scheme, $T_c=T_h/2$.

This problem was solved using different methods. Yuen et al. [30], who treated the radiation problem by a generalized exponential integral function and the coupled problem by one empirical additive approach. Also Kim et al. [28], solved the same problem by using the DOM with S_4 angular quadrature, diamond spatial scheme and uniform grid for the radiative part of the problem while the conductive term is discretized using the central difference scheme. Sakami et al. [31] in their solution of the above problem used a modified discrete ordinates method based on the incorporation of directional ray propagation relations within the cells with triangular grids and in the conduction part of the coupled problem they used the finite element technique. In a similar way Rousse et al. [22], used the control volume method in the radiative part and coupled with the finite element method in energy equation and adopted triangular grids. The method adopted in the present work is simple and can be used to handle combined heat transfer problems in Cartesian space with non-uniform grids. It can also be used to couple with control volume algorithms used in fluid dynamics. The use of non-uniform grid in this case permits more accurate calculation in the sub-domains where more accuracy is needed (by example near of the walls) without additional computational time.

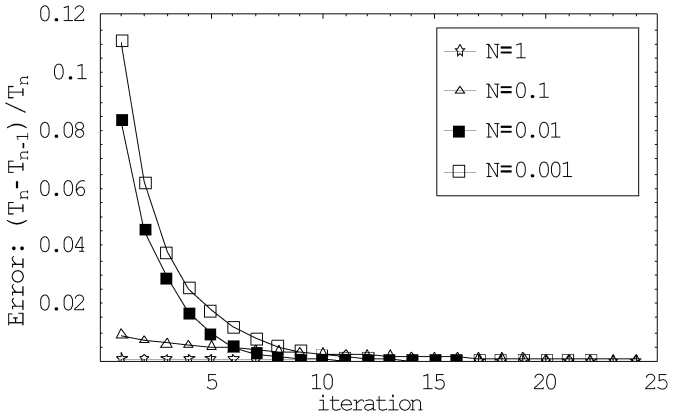

Fig. 3. Comparison of the solution convergence for angular quadrature $LC11$, for $N = 1.0$; 0.1; 0.01; 0.001. Uniform grid.

In this part of the work, the DOM is used with a non-linear high order interpolating scheme called genuinely multidimensional (GM) of Balsara [16] which was used for the case of rectangular uniform grids in radiative problem [27], and is extended here to use with rectangular non-uniform grids. The GM scheme is used because in all the numerical simulations realized in the RTE solution, no negatives intensities were found in iterative process, Balsara [16]. Also, the accuracy of different angular quadratures such S_4, $Tn6$, and the $LC11$ angular quadrature is investigated.

The results are shown for several values of Planck number $N = k\beta/4\sigma_o T_h^3$, where k is the thermal conductivity of the medium and σ_o is the Stefan–Boltzmann constant. The results from [22,28,30,31] show good agreement for $N > 0.01$, wherever for $N \leqslant 0.01$ the results of Yuen et al. [30], shows no agreement with the other authors.

It was found that the numerical solution of the energy equation needs a relaxation factor (λ) to obtain convergence. This is important for lower N values. Fig. 3 shows the variation of error for different values of N for the case of 20×20 uniform grid. One can observe that for the lowest N value the convergence of the algorithm is less quick, meanwhile in all tested situations the algorithm was efficient. Fig. 4 shows the convergence curves for $N = 0.01$ for 20×20 non-uniform grid cases where the logarithm scale permits to observe more easily the error variation until achieving convergence. It is worth to mention

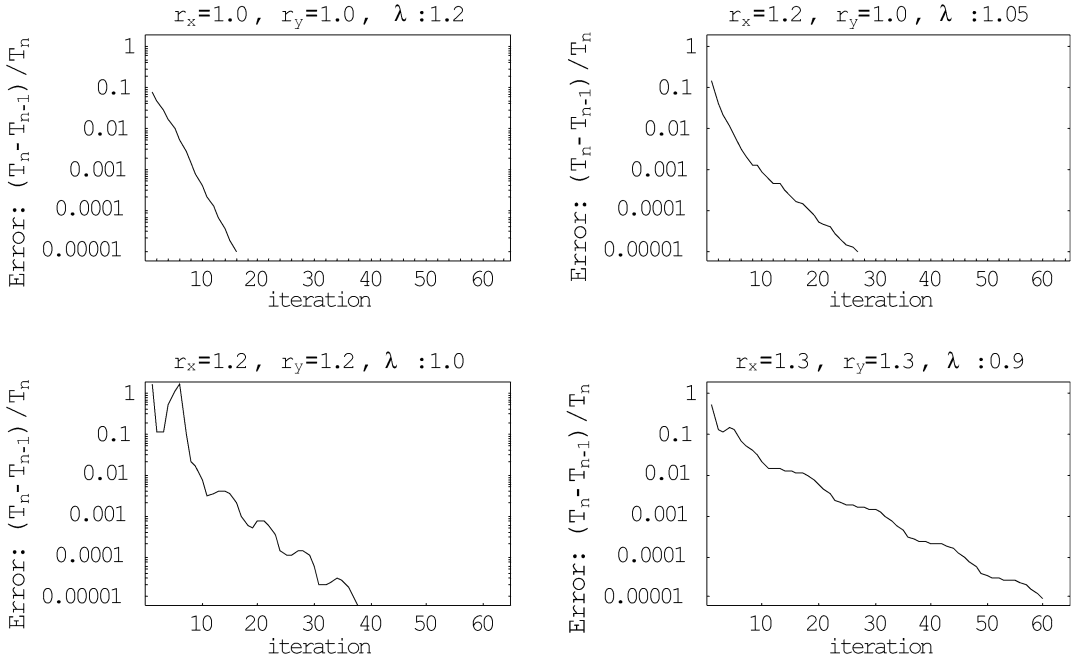

Fig. 4. Comparison of the solution convergence when using uniform and non-uniform grid and relaxation factor, for $N = 0.01$, angular quadrature $LC11$ and $\beta x_L = 1.0$.

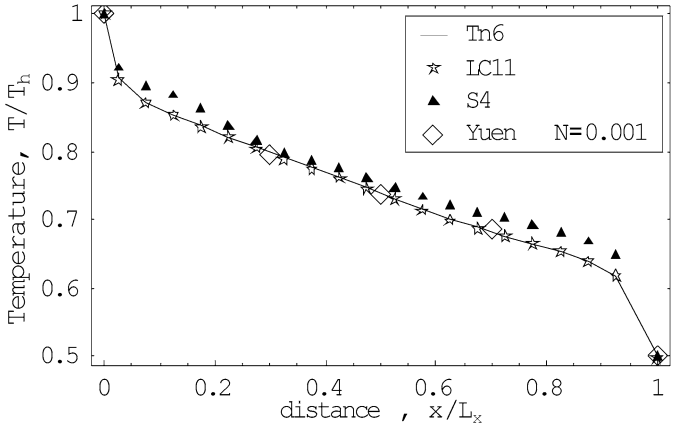

Fig. 5. Comparison of solution convergence for different angular quadratures: T_6, $LC11$ and $S4$; Using uniform grid and relaxation factor and for $N = 0.001$ and $\beta x_L = 1.0$.

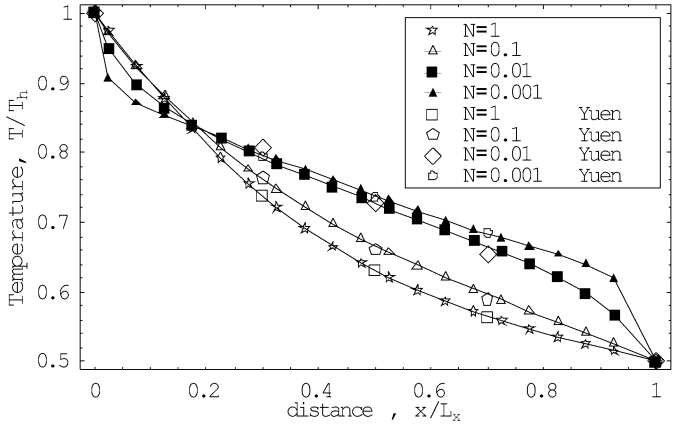

Fig. 6. Comparison of the non-dimensional temperatures distribution in the medium, in section $y = y_L/2$, with the solution of Yuen et al. (1988), for Planck number $N = 1.0$; 0.1; 0.01; 0.001, and $\beta x_L = 1.0$.

that obtaining a fast converged solution does not always means accuracy of solution and it frequent to find that less order angular quadrature converges fast but usually with poor accuracy. In the case of uniform grids one can see that in some cases it converges faster that non-uniform grid but with less accuracy near the boundaries for the grid (by example 20×20 grid). It is found that for values of r_x and r_y near of 1.0 one can use over relaxation $\lambda > 1$, but for higher values of r_x and r_y the solution requires lower values of the relaxation factor $\lambda < 1$, due to the initial instability of solution in the iterative process. The non-uniform grid can be used in applications where it is necessary to used refined grid near to boundaries. For example for the 20×20 grid, when using $r_x = 1.2$ the cell near to the west wall is 0.0192 m width and when using $r_x = 1.0$ the cell near of west wall is 0.05 m width. Hence to obtain the same refined grid near the wall it will be necessary to use a 50×50 uniform grid, requiring lot of memory and CPU time.

The solution convergence for different angular quadratures was also investigated. The quadrature $LC11$ proposed by Lededev in [19] and recommended by Koch et al. [19], with 48 directions in 2D is included here with the S_n and T_N quadratures. Fig. 5 shows the comparison of the numerical solution for $N = 0.001$, for $Tn6$, $LC11$ and $S4$ quadratures. One can observe that the agreement between the numerical results for $Tn6$ and $LC11$ quadratures is good and agree well with results of Yuen et al. [30] and Sakami et al. [31]. While poor agreement is found for the S_4 numerical results. The use of $LC11$ quadrature permits reducing approximately to $1/3$ the computational time of the $Tn6$ quadrature.

Fig. 6 shows the temperature distribution in the medium for Planck number N, between 0.001 and 1.0 when using 20×20 uniform grid. The results show good agreement with those of Kim et al. [28], Yuen et al. [30] and Sakami et al. [31]. As N decreases, the role of the radiation increases, and the energy is transmitted deeper into the medium, producing higher temperature gradients at both faces and increasing temperatures near the cold face. Fig. 7(a) shows the comparison of the temperature distribution at $L_y/2$ for different non-uniform grid with the results for uniform grid. It appears that the solutions are in

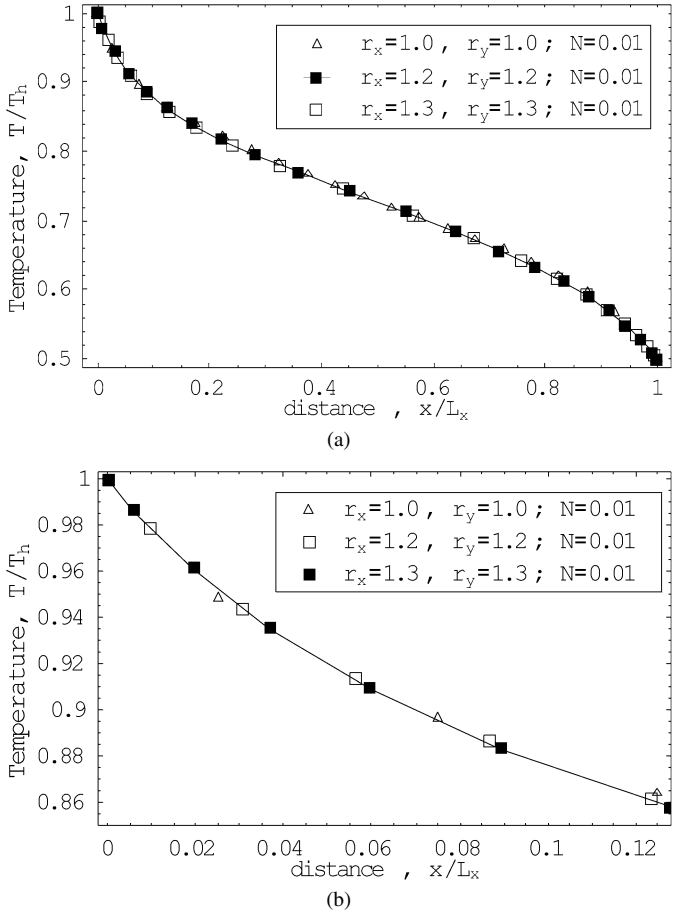

Fig. 7. Comparison of the non-dimensional temperatures distribution in the medium, in section $y = y_L/2$, for uniform and non-uniform grid modeling; quadrature $LC11$ and $\beta x_L = 1.0$.

good agreement. Fig. 7(b) shows the comparison of the temperature distribution near the hot wall in section $L_y/2$ for uniform and non-uniform grids. It is found that non-uniform grid solution for $r_x = r_y = 1.2$ and for $r_x = r_y = 1.3$ are close to each other, and the points of uniform grid solution case show some difference with respect to those results near the wall. To show the conservation of the heat flux, calculations of the total, ra-

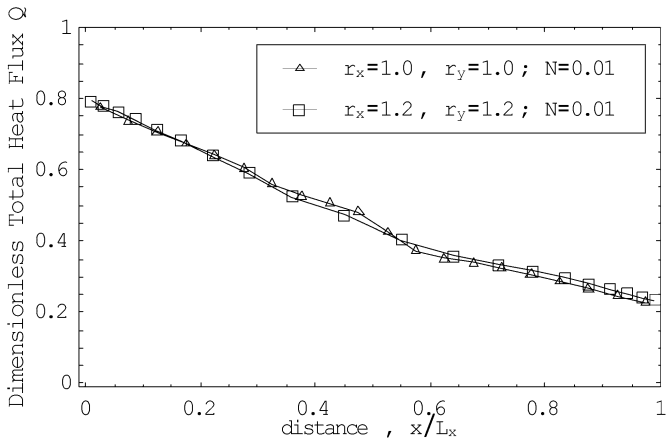

Fig. 8. Comparison of the non-dimensional total heat flux distribution in the medium, in section $y = y_L/2$, for uniform and non-uniform grid modeling; quadrature $LC11$ and $\beta x_L = 1.0$.

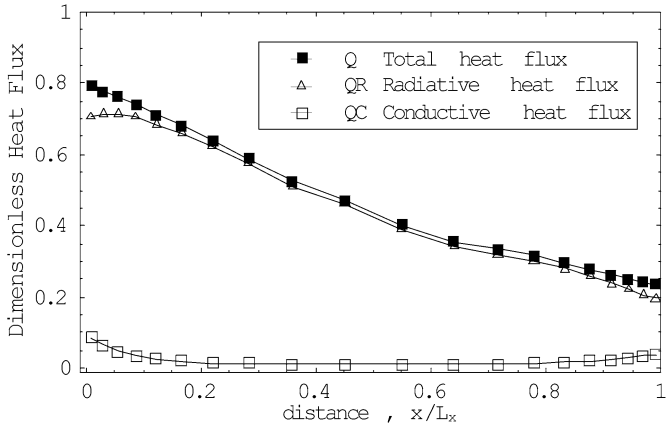

Fig. 9. Comparison of the dimensionless total, radiative and conductive heat flux distribution in the medium, in section $y = y_L/2$, for $N = 0.01$; grid: $r_x = 1.2$, $r_y = 1.0$; quadrature $LC11$ and $\beta x_L = 1.0$.

diative and conductive heat fluxes are realized in the medium. Fig. 8 shows the comparison of non-dimensional total heat flux distribution in the medium at the symmetry line $Y = 0.5$ for $N = 0.01$, when using uniform grid and non-uniform grid. In both cases the results are in agreement with the results reported by Kim et al. [28], and it is appears that the non-uniform curve is more smooth. The $N = 0.01$ case is selected here because it is more non-linear than other higher N values. Fig. 9 shows the variation of radiative and conductive heat fluxes along the x-direction at $Y = 0.5$. It is observed that the curves are smooth and no heat flux inconsistencies are found by the use the non-uniform grid. Also, it can be observed that for $N = 0.01$, the radiative mode is predominant and conductive effects are more important near the walls. Fig. 10 shows the comparison of the total heat distribution on the hot wall for $N = 0.01$ and non-uniform grid with the results of Sakami et al. [31] for the case of pure absorption which is equal to case of pure scattering ($\omega = 0$). The results show no significant discrepancy with respect to those of Kim et al. [28] and Sakami et al. [31]. Fig. 11 shows the non-uniform grid lines and the isotherms

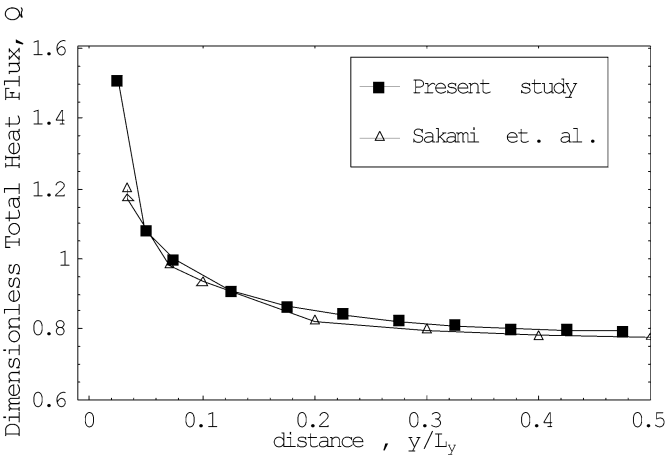

Fig. 10. Dimensionless total heat flux distribution on the hot wall, $x = 0$, for $N = 0.01$; grid: $r_x = 1.2$, $r_y = 1.0$; quadrature $LC11$ and $\beta x_L = 1.0$.

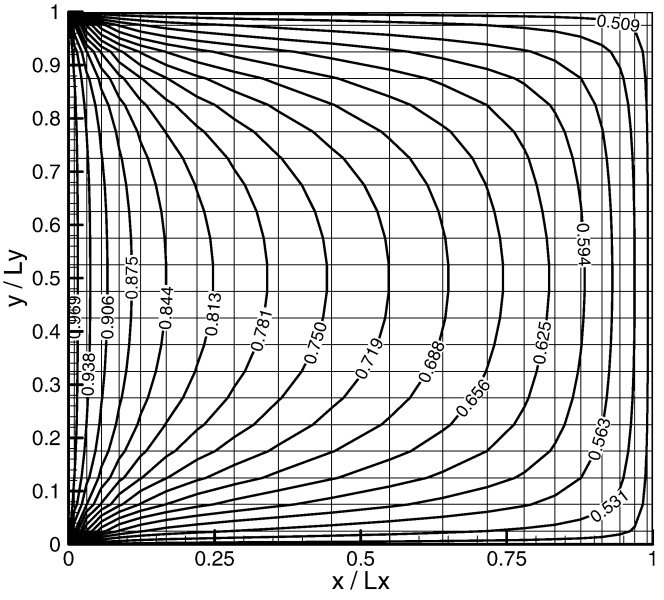

Fig. 11. Non-dimensional temperature distribution in the medium using non-uniform grid: $r_x = 1.2$, $r_y = 1.0$; $N = 0.01$; quadrature $LC11$ and $\beta x_L = 1.0$.

in the medium for the case of $T_c = T_h/2$ illustrating smooth isotherms curves in all domain.

The method is tested for high gradient temperature case, and Fig. 12 shows the total, radiative and conductive heat fluxes on the hot wall for the case of $T_c = T_h/3$ for $N = 0.01$ and non-uniform grid. In this case, even the radiative mode is predominant near the wall. Fig. 13 shows the isotherms in the medium for the same case of $T_c = T_h/3$, and one can be observe the smooth variation of temperatures in the medium. It is found that the method and the algorithm used are adequate when used in high temperature gradient cases.

7. Conclusions

In this study the multidimensional scheme (GM) in the classical discrete ordinates method is found to be suitable for accurate calculations of radiative transfer with non-uniform grids.

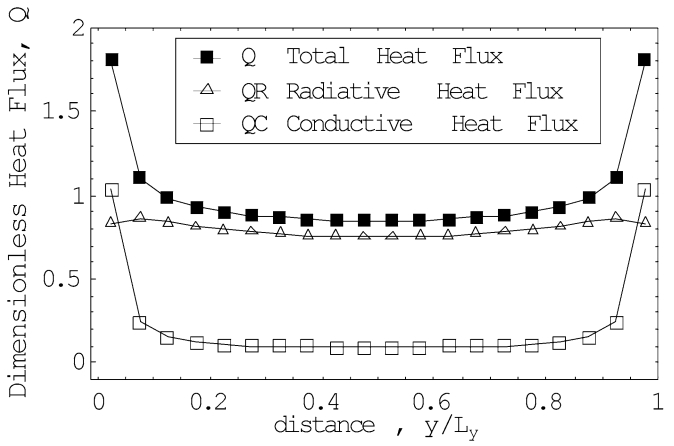

Fig. 12. Comparison of the dimensionless total, radiative and conductive heat flux distribution on the hot wall, $x = 0$, for case $T_c = T_h/3$, and $N = 0.01$; grid: $r_x = 1.2$, $r_y = 1.0$; quadrature $LC11$ and $\beta x_L = 1.0$.

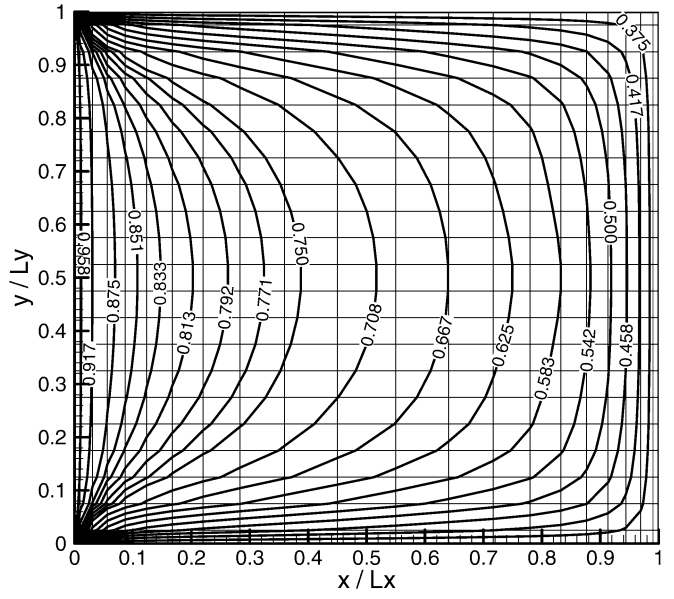

Fig. 13. Non-dimensional temperature distribution in the medium for case $T_c = T_h/3$, using non-uniform grid: $r_x = 1.2$, $r_y = 1.0$; $N = 0.01$; quadrature $LC11$ and $\beta x_L = 1.0$.

Also, it is found that with GM, it was not necessary to use the common technique to set zero negative intensities which that eliminate one possible important error source in programming code. The algorithm is used in radiation–conduction case and the results are shown to be accurate. For higher values of r_x and r_y, it is necessary to use a lower relaxation value. The method used in this work is simple and is useful for to handle combined heat transfer problems in Cartesian space with non-uniform grids and can to used coupled with common volume control algorithms used in fluid dynamics. The use of non-uniform grid in this case permits accurate calculation in the sub-domains where more accuracy is needed (near of the walls) without additional computational time.

Acknowledgements

The authors wish to thank the CNPQ for the scholarships.

References

[1] M. Krook, On the solution of equations of transfer – I, Astrophys. J. 122 (3) (1955) 488–497.
[2] P. Cheng, Two-dimensional radiating gas flow by a moment method, AIAA J. 2 (1964) 1662–1664.
[3] S. Chandrasekhar, Radiative Transfer, Clarendon Press, Oxford, 1950.
[4] K.D. Lathrop, B.G. Carlson, Discrete ordinates angular quadrature of the neutron transport equation, Technical Information Series Report LASL-3186, Los Alamos Scientific Laboratory, 1965.
[5] K.D. Lathrop, Use discrete ordinates methods for solution of photon transport problems, Nucl. Sci. Engrg. 24 (1966) 381–388.
[6] W.A. Fiveland, Discrete ordinates solutions of the radiative transport equation for retangular enclosures, Trans. ASME J. Heat Transfer 106 (1984) 699–706.
[7] W.A. Fiveland, Three-dimensional radiative heat transfer solutions by the discrete ordinates method, J. Thermophys. Heat Transfer 2 (1988) 309–316.
[8] R. Viskanta, M.P. Menguc, Radiation heat transfer in combustion systems, Prog. Energy Combust. Sci. 13 (1987) 97–160.
[9] M.A. Ramankutty, A.L. Crosbie, Modified discrete ordinates solution of radiative transfer in two-dimensional rectangular enclosures, J. Quant. Spectrosc. Radiat. Transfer 57 (1997) 107–140.
[10] M.A. Ramankutty, A.L. Crosbie, Modified discrete ordinates solution of radiative transfer in three-dimensional rectangular enclosures, J. Quant. Spectrosc. Radiat. Transfer 60 (1998) 103–134.
[11] M. Sakami, A. Charette, Application of a modified discrete ordinates method to two-dimensional enclosures of irregular geometry, J. Quant. Spectrosc. Radiat. Transfer 64 (2000) 275–298.
[12] B. VanLeer, Towards the ultimate conservation difference scheme II: Monoticity and conservation combined in a second-order scheme, J. Comput. Phys. 14 (1974) 361–370.
[13] A. Harten, High resolution schemes for hyperbolic conservation laws, J. Comput. Phys. 49 (1983) 357–393.
[14] J.P. Jesseee, W.A. Fiveland, Bounded, high resolution differencing schemes applied to the discrete ordinates method, J. Thermophys. Heat Transfer 11 (1997) 47–54.
[15] D. Sidilkover, P.L. Roe, Unification of some advection schemes in two dimensions, Techreports ICASE 1995.
[16] D. Balsara, Fast and accurate discrete ordinates methods for multidimensional radiative transfer. Part I, basic methods, J. Quant. Spectrosc. Radiat. Transfer 69 (2001) 671–707.
[17] J.S. Truelove, Discrete ordinates solutions of the radiation transport equation, Trans. ASME J. Heat Transfer 109 (1988) 1048–1051.
[18] C.P. Thurgood, A. Pollard, H.A. Becker, The T_N quadrature set for the discrete ordinates method, J. Heat Transfer 117 (1995) 1068–1070.
[19] R. Koch, R. Becker, Evaluation of quadrature schemes for the discrete ordinates method, J. Quant. Spectrosc. Radiat. Transfer 84 (2004) 423–435.
[20] M.F. Modest, Radiative Heat Transfer, second ed., Academic Press, New York, 2003.
[21] D.R. Rousse, Numerical predictions of two-dimensional conduction, convection and radiation heat transfer – I. Formulation, Int. J. Therm. Sci. 39 (2000) 315–331.
[22] D.R. Rousse, G. Gautier, J.F. Sacadura, Numerical predictions of two-dimensional conduction, convection and radiation heat transfer – I. Validation, Int. J. Therm. Sci. 39 (2000) 332–353.
[23] K.H. Lee, R. Viskanta, Two-dimensional combined conduction and radiation heat transfer: comparison of the discrete ordinates method and the diffusion approximation methods, Numer. Heat Transfer Part A 39 (2001) 205–225.
[24] D. Lacroix, G. Parent, F. Asllanaj, G. Jeandel, Coupled radiative and conductive heat transfer in a non-grey absorbing and emitting semitransparent media under collimated radiation, J. Quant. Spectrosc. Radiat. Transfer 75 (2002) 589–609.
[25] P. Talukdar, S. Mishra, Analysis of conduction–radiation problem in absorbing emitting and anisotropically scattering media using the collapsed dimension method, Int. J. Heat Mass Transfer 45 (2002) 2159–2168.

[26] R. Siegel, J.R. Howell, Thermal Radiation Heat Transfer, third ed., Taylor & Francis, London, 1992.
[27] K.A.R. Ismail, C.T.S. Salinas, Application of multidimensional scheme and the discrete ordinate method to radiative heat transfer in a two-dimensional enclosure with diffusely emitting and reflecting boundary walls, J. Quant. Spectrosc. Radiat. Transfer 88 (2004) 407–422.
[28] T.Y. Kim, S.W. Baek, Analysis of combined conductive and radiative heat transfer in a two-dimensional rectangular enclosure using the discrete ordinates method, Int. J. Heat Mass Transfer 34 (1991) 2265–2273.
[29] S.V. Patankar, Numerical Heat Transfer and Fluid Flow, Hemisphere, Washington, DC, 1980.
[30] W. Yuen, E. Takara, Analysis of combined conductive-radiative heat transfer in a two-dimensional rectangular enclosure with a gray medium, Trans. ASME J. Heat Transfer 110 (1988) 468–474.
[31] M. Sakami, A. Charette, V. Le Dez, Application of the discrete ordinates method to combined conductive and radiative heat transfer in two-dimensional complex geometry, J. Quant. Spectrosc. Radiat. Transfer 56 (1996) 517–533.